Computer Aided Multi-Parameter Extraction System to Aid Early Detection of Skin Cancer Melanoma

Ruksar Fatima[†], **Mohammed Zafar Ali Khan** [††], **A. Govardhan**[†††] **and Kashyap D Dhruve***

[†] *Head Dept of Bio-Medical Engg, KBN College Of Engg, Gulbarga, Karnataka*
[††] *Associate Professor & Head of the Department IIT Hyderabad, Hyderabad, India*
[†††] *Registrar of Evaluation of JNTU, Hyderabad, India.*
* *Technical Director, Planet-i Technologies, Bangalore, India*

Summary
Melanoma is the most widely occurring and life threatening form of skin cancer. Early detection of in situ melanoma has challenged researchers for many decades now. Currently there exists no computer aided mechanisms to accurately detect early melanoma. The currently existing computer aided diagnostics mechanisms are capable of melanoma classification and are unable to detect in situ melanoma. This paper introduces a Multi Parameter Extraction and Classification System ($MPECS$) to aid early detection of skin cancer melanoma. The $MPECS$ defines the skin lesion images in terms of characteristic parameters which are further used for classification. In this paper the extraction of 21 parameters is achieved using a six phase approach. The parameters extracted are analyzed using statistical methods. It is clear from the results obtained that no single parameter can affirm the detection of in situ melanoma, hence an advanced analysis mechanisms considering all the parameters need to be adopted to effectively detect melanoma in its initial stages.

Key words:
Skin Cancer, Melanoma, Early Detection, In Situ Melanoma, $MPECS$ *, Multi Parameter Extraction, Classification, Computer Aided Diagnostics, Image Processing, Skin Lesions. Feature Extraction.*

1. Introduction

Skin Cancer Melanoma derives its name from Melanocytes. Melanocytes are cells that induce a brown pigmentation in the skin. Generally biopsy's are performed by dermatologists to ascertain the existence of melanoma. A recent survey conducted in the United States of America[1] estimates 12,190 deaths in the current year owing to skin cancer ailments. Out of the 12,190 deaths, melanoma accounts for 9,180 deaths i.e. 75.3%. Melanoma Skin Cancers have also seen an enhanced number of cases [2][3] in India and worldwide[4][5]. Exposure to Ultraviolet rays is a major factor aiding the growth of skin cancers. Skin cancer melanoma and especially cutaneous melanoma that occurs most commonly is yet incurable and life threatening. Early diagnostics of melanomas enables fruitful treatment and cure. To enable early detection of skin cancers generally invasive procedures like biopsies are performed. Non invasive procedure are preferred means of diagnostics. Studies also prove the complexity of early diagnosis by even "Primary Care Physicans" [6]. The recent decade has seen an increased adoption of computer aided diagnostics mechanisms to support skin lesion characterization and assessment [7]. Researchers working in the arena of Dermatology imagining have put forth that the diagnosis of skin melanomas is achievable by extraction of the color features and physical features of skin lesions [8]. The use of advanced imaging technologies like optical coherence tomography [9] and confocal microscopy [10] have also been proposed by researchers to develop computer aided diagnostics systems. The advanced imagining technologies though accurate are expensive and require experienced personnel for operational procedures [11].

It is well understood that there exists a need to develop non invasive computer aided diagnostics systems to enable early detection of skin cancer melanoma utilizing non expensive imaging systems. This paper introduces the $MPECS$ to enable early detection of in situ melanoma. The diagnostic system proposed adopts a multi phase parameter extraction procedure to define the skin lesions under test and doctrines the use of these parameters to classify the skin lesions into primarily three categories i.e. Melanoma Lesions, Early Melanoma Lesions and Non Melanoma Lesions. The research work presented through this paper also discusses the statistical analysis of the parameters extracted.

The manuscript is organized as follows. The second section discusses the literature review carried out during the course of the research presented here. The next section introduces the $MPECS$ proposed and the phase wise approach adopted to extract the parameters. The dataset creation used to evaluate the $MPECS$ and the statistical analysis is explained in the penultimate section of this paper. The conclusion and future work is discussed in the fifth section of this paper.

Manuscript received October 5, 2012
Manuscript revised October 20, 2012

2. Literature Review

The conventional and the most commonly used methodology to detect skin cancer melanoma are based on the Asymmetry Border Color and Differential Structure ($ABCD$) rules [12]. The $ABCD$ principle has been adopted by various researchers to develop classification systems. The $ABCD$ systems have been optimized to include additional algorithms like "$JSEG$" [13] , hybrid approaches [14] using edge detection and color transformation and , fuzzy based optimizations [15] for border detection . The use of wavelet decomposition techniques and the $ABCD$ rule based classification system exhibits a classification accuracy of 60% which betters the classification accuracy achieved by the $ABCD$ rule alone [16]. The major drawback of such systems is that these exhibit a low classification accuracy and cannot be adopted for early detection of skin cancer melanoma. Apart from the $ABCD$ rule method researchers have also adopted the Menzies Method [15] and the Seven Point check list method [17][18]. The seven point check list method exhibits better classification efficiency than the $ABCD$ rule based systems but the Menzies and the seven point check list method are sparingly used for classification of skin lesions owing to the complexity [7]. Neighboring grey level dependence matrix and lattice aperture waveform set are skin lesion texture based classification systems [19]. The parameters obtained the texture based features were found to be inefficient to accurately classify and recognize early signs of skin cancer melanoma. A comprehensive review of the varied approaches introduced by researchers is carefully studied during the course of research presented here [7].
The existing mechanisms could be adopted to classify skin cancer melanoma but fail to detect and recognize signs exhibited by in situ melanoma which is critical and required for effective preventive care diagnosis.

3. Multi Parameter Extraction and Classification System (MPECS) Modeling

Melanoma skin cancers are till date incurable and owing to this fact they account for the highest amount of deaths amongst skin cancers. These unfortunate occurrences could be avoided if the skin lesion could be diagnosed at early stages which some physicians overlook. Skin Lesions developed could be easily mistaken as other skin related ailments/ cancers if not properly diagnosed. The Multi Parameter Extraction and Classification System ($MPECS$) for skin lesions proposed in this paper is our effort towards enabling the early detection of Skin Cancer Melanoma.

3.1 MPECS – Preliminary Notation

Let's consider a set of dermoscopic skin lesion images for analysis and is represented as

$$I_{SK} = \{i_1, i_2, i_3, i_4, \dots \dots i_n\}$$

Where
i represents an image

n represents the total number of images to be analyzed.

The primary goal of the of the $MPECS$ system proposed in this paper is to enable early diagnosis of skin cancer melanoma skin lesions. Let the classification set be represented as

$$C = \{c_1, c_2, c_3 \dots c_{cl}\}$$

Where cl represents the total number of classes represented by c.

It could be stated that $\forall\, i \in I : \exists!\, c \in C \mid i \in c$.

This paper discusses the multi parameter extraction algorithms adopted for effective classification enabling early detection of skin cancer melanoma. Let the Parameter set be defined by

$$P = \{p_1, p_2, p_3, \dots p_a\}$$

Where a represents the total number of p parameters

In the $MPECS$ an image $i \in I$ is represented by a set of parameters P is used for classification. The image I_n could now defined as

$$I_n = \{p_{n1}, p_{n2}, p_{n3}, \dots p_{np}\}$$

An image I_n could be represented as a matrix and is defined as

$$I_n = \begin{bmatrix} x_{0,0} & \cdots & x_{0,Wd} \\ \vdots & \ddots & \vdots \\ x_{Ht,0} & \cdots & x_{Ht,Wd} \end{bmatrix}$$

Where Ht represents the height and Wd represents the width of the image I_n and x represents the pixel value at the given location.

The $MPECS$ adopts a 6 phase approach to extract the parameters set $P \,\forall\, i \in I_{SK}$. The system considers 21 parameters for classification i.e. $a = 21$. Each phase provides towards the construction of the parameter set P.

3.2 MPECS – Phase 1

This preliminary phase is primarily designed towards identifying the skin lesions present in an image $i \in I$ and extracting the Lesion Borders, the symmetry of the lesions and the color spreading factor of the skin lesions.

To extract the parameters discussed the images are resized using a bicubic interpolation technique. The bicubic interpolation technique is an weighted average of the pixels in the nearest $[4 \times 4]$ proximity and is defined as

$$P_{R\delta z}{}^{i_n}(x,y) = \sum_{i=1}^{3}\sum_{j=1}^{3}\left(wt_{ij} \times x^i y^j\right)$$

Where x, y represent the pixel position and wt_{ij} is the weight at position i, j of the image $i_n \in I_{SK}$

Grey scaling is performed on the resized pixels, and the resultant grey scale pixel is computed based on the following definition.

$$P_{GreyScale}{}^{i_n}(x,y) = \left[0.2989 \times R\left(P_{R\delta z}{}^{i_n}(x,y)\right)\right] + \left[0.5870 \times G\left(P_{R\delta z}{}^{i_n}(x,y)\right)\right] + \left[0.11400 \times B\left(P_{R\delta z}{}^{i_n}(x,y)\right)\right]$$

Where $R\left(P_{R\delta z}{}^{i_n}(x,y)\right)$ represented the red channel value, $G\left(P_{R\delta z}{}^{i_n}(x,y)\right)$ represents the green channel value and $B\left(P_{R\delta z}{}^{i_n}(x,y)\right)$ represents the blue channel value of the resized pixel $P_{R\delta z}{}^{i_n}(x,y)$.

Binirization is performed on the grayscale image utilizing the adaptive thresholding algorithm. The image noise elimination property of the adaptive thresholding based binirazation algorithm is an additional parameter for adopting this algorithm. The adaptive thresholding based binirazation is an iterative process wherein the thresholds are adapted based on the regions it is being performed on. The iterative process is terminated when convergence is achieved. Let $P_{Bin}{}^{i_n}(x,y)$ represent the pixels of the binirized image i_n . The regions of interest (roi) is extracted using the connected component labeling algorithm. The $roi's$ obtained hold the information required and are identified by labels $L_{ROI-l}{}^{i_n}$. The image $i_n \in I_{SK}$ based on the ROI's is defined as

$$i_{n-roi} = \{L_{roi-1}{}^{i_n} \cup L_{roi-2}{}^{i_n} \cup L_{roi-3}{}^{i_n} \cup \cdots \cup L_{roi-l}{}^{i_n}\}$$

Where l represents the total number of $roi's$ extracted.

The centroids of the $roi's$ are computed based on the area enclosed by the $roi's$. The centroids are computed to cluster the similar $roi's$ together in the same vicinity as it is observed that the $roi's$ are similar in nature and can be clustered not effecting the classification accuracy. This operation adopted enables $roi's$ exhibiting similar properties to be clustered into a single cluster together represented as ROI. The labels $L_{roi-l}{}^{i_n}$ used to address the $roi's$ are clustered based on the energy computed and is defined as

$$\mathcal{E}gy_{ROI-l}(L_{ROI-l}{}^{i_n}) = \sum_{pos}\left[\sum_{l \in S_{roi}} \Delta(L_{roi-a}{}^{i_n}, L_{roi-b}{}^{i_n})\right]$$

Where $\Delta(L_{roi-a}{}^{i_n}, L_{roi-b}{}^{i_n})$ represents a function $\Delta(L_{roi-a}{}^{i_n}, L_{roi-b}{}^{i_n}) = \{0,1\}$ i.e. if the $roi's$ $L_{roi-a}{}^{i_n}$ and $L_{roi-b}{}^{i_n}$ are similar, 0 is returned and 1 in the case of dissimilarity. $S_{roi} = \{1,2,3, \ldots . l\}$ represents the set of $roi's$ obtained and $a \in S_{roi}$ and $b \in S_{roi}$. pos represents the position of the l^{th} clustered ROI represented as $L_{ROI-l}{}^{i_n}$.

The clustered $ROI's$ obtained define the image i_n as

$$i_{n-ROI} = \{L_{ROI-1}{}^{i_n} \cup L_{ROI-2}{}^{i_n} \cup L_{ROI-3}{}^{i_n} \cup \cdots \cup L_{ROI-l}{}^{i_n}\}$$

Sobel edge detection is performed on the image $i_{n\ ROI}$. Post the edge detection the distortion on the basis of the coordinate displacement and the frequency of distortion observed is computed using the Fast Fourier Transforms. The axis based asymmetry parameter of the lesion is obtained based on the principal component decomposition. The skin lesion extracted is rotated such that the principal component coincides with the horizontal axis. The skin lesion axis based asymmetry parameter is defined as

$$p_{Axis\_Symmetry} = \left[\sum |i_n(x) - \overline{i_n}(x)|\right] / \left[\sum i_n(x)\right]$$

Where $i_n(x)$ is the original skin lesion and its reflected version is represented as $\overline{i_n}(x)$.

The symmetry parameter is computed for all the pixels within the lesion along the horizontal and vertical axis respectively. The color spreading factor of the lesions is computed based on the similarity of a pixel in a $n \times n$ neighbourhood. The standard deviation of the pixels in the neighborhood based on the Red channel, Green channel and Blue channel is computed using

$$\sigma_{Chnl} = \sqrt{\frac{1}{n^2}\sum_{i=1}^{n^2}(Chnl_i - \overline{Chnl})^2}$$

Where $Chnl = \{R_{Chnl}, G_{Chnl}, B_{Chnl}\}$ and $\overline{Chnl}$ represents the mean value defined as

$$\overline{Chn} = \frac{1}{n^2}\sum_{i=1}^{n^2} Chn_i$$

The cumulative standard deviation for all the channels is defined as

$$\sigma_{Cumilitive} = \sigma_{R_{Chnl}} + \sigma_{G_{Chnl}} + \sigma_{B_{Chnl}}$$

$$\sigma_{Cumilitive} = \left[\sqrt{\frac{1}{n^2}\sum_{i=1}^{n^2}(R_{Chnl_i} - \overline{R_{Chnl}})^2}\right] + \left[\sqrt{\frac{1}{n^2}\sum_{i=1}^{n^2}(G_{Chnl_i} - \overline{G_{Chnl}})^2}\right] + \left[\sqrt{\frac{1}{n^2}\sum_{i=1}^{n^2}(B_{Chnl_i} - \overline{B_{Chnl}})^2}\right]$$

The color spreading factor of the lesion is computed using

$$p_{Clr-Spread} = 1 - \sigma_{Norm}$$

Where σ_{Norm} is the normalized value of $\sigma_{Cumilitive}$ between the range 0 and 1 and is obtained as

$$\sigma_{Norm} = \sigma_{Cumilitive} / \sigma_{Cumilitive-Max}$$

In order to extract the lesion border parameters the image is filtered using the Gaussian and laplacian filter. The parameter describing the lesion borders is obtained by computing the mean of the resultant pixels and is defined as

$$p_{Lesion-Boundry} = \left[\sum_{x=1}^{Wd}\sum_{y=1}^{Ht} P^{i_n}(x,y)\right] \Big/ [Wd \times Ht]$$

In this phase the parameters of the lesions such as the assymmetry along the horizontal and vertical axis , the color spreading factor of the lesion and the boundary parameters is discussed.

3.3 MPECS – Phase 2

The second phase of the $MPECS$ enables the extraction of the area, perimeter and the eccentricity. This phase considers the binirized and clustered ROI image as an input and computes the parameters based on the binirized image obtained from phase 1 defined as

$$i_{n-ROI} = \{L_{ROI-1}{}^{i_n} \cup L_{ROI-2}{}^{i_n} \cup L_{ROI-3}{}^{i_n} \cup \cdots \cup L_{ROI-l}{}^{i_n}\}$$

Where l represents the total number of $ROI's$ identified for the image i_n .

The $ROI's$ of image i_{n-ROI} contain binirized pixel points i.e. black or white pixels. The area parameter defines the white pixels that are encapsulated by the skin lesion and the lesion area parameter is computed using

$$p_{Lesion-Area} = (1/2)\left[\, \left| \sum_{i,j=0}^{Pnts-1} \left(x_i y_{j+1} - x_{i+1} y_j\right) \right| \,\right]$$

Where $Pnts$ is the number of points enclosed by the skin lesion defined by the l^{th} ROI . Also i, j represent the $Pnts$ location and $(x_i, y_j) \in \{ (x_i, y_j) \mid f(x_i, y_j) = 1 \}$ as x_i, y_j represents a white pixel.

The perimeter defines the boundary ΔB length of the skin lesion. The lesion boundary is computed using

$$\Delta B(l) = (B(2{:}\,l,:) - B(1{:}\,l-1,:))^2$$

Where l represents the number of $ROI's$ and its corresponding boundary is represented as B.

The parameter defining boundary of the skin lesion is defined as

$$p_{Lesion-Bound} = \sum \sqrt{\sum_{l} \Delta B(l)}$$

The aspect ratio of the skin lesion is defined as the eccentricity of a skin lesion. The eccentricity is obtained by obtaining the moments represented as M. The major axis is defined as

$$A_{Major} = 2\sqrt{2}(\sqrt{M_{xx} + M_{yy} + M_{Comm}})$$

The minor axis is defined as

$$A_{Minor} = 2\sqrt{2}(\sqrt{M_{xx} + M_{yy} - M_{Comm}})$$

Where the moments M_{xx} , M_{yy}, M_{xy} and M_{Comm} are defined as

$$M_{xx} = \left[\left(\sum x^2\right)/N + 1/12\right]$$

$$M_{yy} = \left[\left(\sum y^2\right)/N + 1/12\right]$$

$$M_{xy} = \left[\left(\sum x * y\right)/N\right]$$

And

$$M_{Comm} = \sqrt{(M_{xx} - M_{yy})^2 + 4{M_{xy}}^2}$$

The eccentricity parameter is computed using

$$p_{Lesion-Eccent} = \left[\sqrt[2]{\left({A_{Major}}^2 - {A_{Minor}}^2\right)}\right]/A_{Major}$$

3.4 MPECS – Phase 3

Researches have well understood the importance to 3D depth parameters to enhance the classification accuracy [22][23]. To obtain the 3D depth of the skin lesions the $MPECS$ introduced in this paper considers creating a 3×3 masked windows represented as

$$i_{n_{3\times3-Mask}} = \begin{bmatrix} W_1 & W_2 & W_3 \\ W_4 & W_5 & W_6 \\ W_7 & W_8 & W_9 \end{bmatrix}$$

Where W_i represent the weights of the pixel

The projection filter is defined as

$$i_{n_{3D-Depth}} = \sum_{i=1}^{9} W_i I_i$$

Where I_i represents the intensity of the i^{th} pixel.

The 3D depth projection parameter $p_{Lesion-3DDept}$ is obtained by considering the geometric mean defined as

$$\begin{aligned} p_{Lesion-3DDept} = {} & [1/9] \\ & \times \left[I_{x-1,y-1} + I_{x-1,y1} + I_{x-1,y+1} \right. \\ & + I_{x,y-1} + I_{x,y} + I_{x,y+1} + I_{x+1,y-1} \\ & \left. + I_{x+1,y1} + I_{x+1,y+1}\right] \end{aligned}$$

Where x, y represent the horizontal and vertical pixel position.

3.5 MPECS – Phase 4

The fourth phase of the $MPECS$ is targeted towards obtaining the color components of the skin lesions. The color components are extracted for the red channel blue channel and the green channel. The mean and the variance parameters of each channel are considered as the parameters to be utilized for classification. For the red channel the mean parameter is defined as follows

$$p_{RChnl-Mean} = \frac{\sum_{x=1}^{Wd} \sum_{y=1}^{Ht} R_{Chnl}(x, y)}{Wd * Ht}$$

Where x, y represent the pixel positions.

The variance parameter is computed by obtaining the mean of all the coluB_{Chnl}mns , the difference amongst them and then summed square difference divided by the height Ht

$$Clm\_mean_{RChnl}(i) = \frac{\sum_{i=1}^{Wd} R(i)}{Wd}$$

$$Diff_{RChnl}(i) = RChn(:, i) - Clm\_mean_{RChnl}(i)$$

$$p_{RChnl-Var} = \frac{\sum_i Diff_{RChnl}(i)}{(Ht - 1)}$$

Similarly the green channel and blue channel parameters are defined as

$$p_{G_{Chnl}l-Mean} = \frac{\sum_{x=1}^{Wd} \sum_{y=1}^{Ht} G_{Chnl}(x, y)}{Wd * Ht}$$

$$p_{G_{Chnl}-Var} = \frac{\sum_i Diff_{G_{Chnl}}(i)}{(Ht - 1)}$$

$$p_{B_{Chnl}-Mean} = \frac{\sum_{x=1}^{Wd}\sum_{y=1}^{Ht} B_{Chnl}(x,y)}{Wd * Ht}$$

$$p_{B_{Chnl}-Var} = \frac{\sum_i Diff_{B_{Chnl}}(i)}{(Ht-1)}$$

3.6 MPECS – Phase 5

This phase of the $MPECS$ discusses the smoothening process of the $RChnl$ and G_{Chnl} using the 3×3 masking procedure discussed in the third phase. The smoothing is not adopted for the B_{Chnl} as the blue veils of the skin lesions is an important parameter for early detection of skin cancer melanoma [24]. The smoothening filter for the $RChnl$ and G_{Chnl} is defined as follows

$$i_{n_{RChnl-Smooth}} = \sum_{i=1}^{9} W_i RChnl_i$$

$$i_{n_{G_{Chnl}-Smooth}} = \sum_{i=1}^{9} W_i G_{Chnl_i}$$

Where W_i represent the weights of the pixel and $RChnl_i, G_{Chnl_i}$ is red channel intensity and green channel intensity of the i^{th} pixel.

The red channel smoothened parameter $p_{RChnl-Smooth}$ is defined as

$$p_{RChnl-Smooth} = [1/9] \times \left[RChnl_{x-1,y-1} + RChnl_{x-1,y1} + RChnl_{x-1,y+1} + RChnl_{x,y-1} + RChnl_{x,y} + RChnl_{x,y+1} + RChnl_{x+1,y-1} + RChnl_{x+1,y1} + RChnl_{x+1,y+1}\right]$$

The green channel smoothened parameter $p_{G_{Chnl}-Smooth}$

$$p_{G_{Chnl}-Smooth} = [1/9] \times \left[G_{Chnl_{x-1,y-1}} + G_{Chnl_{x-1,y1}} + G_{Chnl_{x-1,y+1}} + G_{Chnl_{x,y-1}} + G_{Chnl_{x,y}} + G_{Chnl_{x,y+1}} + G_{Chnl_{x+1,y-1}} + G_{Chnl_{x+1,y1}} + G_{Chnl_{x+1,y+1}}\right]$$

3.7 MPECS – Phase 6

For early detection of skin cancer melanoma it is essential to extract all the color components of the skin lesion to obtain accurate classification results [20][21]. The $MPECS$ discussed considers the cylindrical coordinate representation of pixels in the fourth and fifth phase. In order to extract accurate and elaborate color parameters this phase of the $MPECS$ considers the Cartesian representation of pixels. Hue, Saturation and Value representation of the pixels are considered as the Cartesian representations. The mean and variance parameters of the hue channel, variance channel and the value channel are extracted from the $R_{Chnl}, G_{Chnl} and B_{Chnl}$ pixel values of the skin lesions. The hue value of a pixel is computed using the following definition

$$Hue_{i,j} = \begin{cases} \left[0 + \frac{43 * |G_{Chnl} - B_{Chnl}|}{MaxVal - MinVal}\right] & , MaxVal = RChnl \\ \left[85 + \frac{43 * |B_{Chnl} - RChnl|}{MaxVal - MinVal}\right] & , MaxVal = G_{Chnl} \\ \left[171 + \frac{43 * |RChnl - G_{Chnl}|}{MaxVal - MinVal}\right] & , MaxVal = B_{Chnl} \end{cases}$$

Where $MaxVal = Max(RChnl, G_{Chnl}, B_{Chnl})$ is the maximum value of the red green and blue channel of the pixel

$MinVal = Min(RChnl, G_{Chnl}, B_{Chnl})$ is the minimum value of the red green and blue channel of the pixel

The Saturation and the value parameter of the pixel is computed using

$$Saturation_{i,j} = 255 * \frac{\{MaxVal - MinVal\}}{MaxVal}$$

$$Value_{i,j} = MaxVal$$

The mean of the hue channel and the is defined as

$$p_{Hue_{Chnl}l-Mean} = \frac{\sum_{x=1}^{Wd}\sum_{y=1}^{Ht} Hue_{Chnl}(x,y)}{Wd * Ht}$$

The variance is computed in a manner similar to the procedure described in phase 4 and is defined as

$$p_{Hue_{Chnl}-Var} = \frac{\sum_i Diff_{Hue_{Chnl}}(i)}{(Ht-1)}$$

The mean and the variance of the saturation channel is defined as

$$p_{Saturation_{Chnl}-Mean} = \frac{\sum_{x=1}^{Wd}\sum_{y=1}^{Ht} Saturation_{Chnl}(x,y)}{Wd * Ht}$$

$$p_{Saturation_{Chnl}-Var} = \frac{\sum_i Diff_{Saturation_{Chnl}}(i)}{(Ht-1)}$$

Accordingly the Value channel parameters are obtained using the following equations

$$p_{Value_{Chnl}-Mean} = \frac{\sum_{x=1}^{Wd}\sum_{y=1}^{Ht} Value_{Chnl}(x,y)}{Wd * Ht}$$

$$p_{Value_{Chnl}-Var} = \frac{\sum_i Diff_{Value_{Chnl}}(i)}{(Ht-1)}$$

The $MPECS$ discussed in this paper discusses the extraction 21 vital parameters which would enable for classification of skin lesions especially targeted towards early detection of skin cancer melanoma. The parameter extraction and the procedure involved in extraction are achieved adopting a six phase approach discussed above. The classification procedure adopted by the $MPECS$ is considered beyond the scope of this paper and is discussed in the subsequent publications related to the research work presented here. The realization of the $MPECS$ and the analysis is discussed in the subsequent section of this paper.

4. Experimental Study of the MPECS

In order to evaluate the parameter extraction and classification of skin lesions a dataset is created from the skin images obtained from the "The Atlas of Dermoscopy" [25]. The interactive atlas of dermoscopy consists of over 2000 skin lesion images. Researcher's have extensively used this as a reference to evaluate their research related to skin cancer melanoma [24][26] Based on the data provided in the atlas the skin lesion images were sorted into three categories namely Advanced Skin Cancer Melanoma, In situ Melanoma Images or early skin cancer melanoma images and skin lesions of other types or non melanoma skin lesions. The $MPECS$ proposed in this paper was evaluated on the custom dataset created from the images provided in the atlas. Matlab was adopted to develop the $MPECS$ parameter extraction. The analysis of the results was carried out using an analysis tool developed on the .Net 2010 platform using C# a the programming language. Let the parameters to be analyzed be represented by the set A_P and the set is defined as follows

$$A_P = \{a_1, a_2, a_3, \dots \dots . a_m\}$$

The analysis results obtained is defined as

$A_{P\text{-Result}}$=\{ A_{P-Sum}, A_{P-Mean}, $A_{P-Geometric\ Mean}$, $A_{P-Harmonic\ Mean}$, A_{P-Min}, A_{P-Max}, $A_{P-Range}$, $A_{P-Variance}$, $A_{P-Standard\ deviation}$, $A_{P-Skewness}$, $A_{P-Kurtosis}$, $A_{P-First\ Quartile}$, $A_{P-Third\ Quartile}$, $A_{P-Median}$, $A_{P-Inter\ Quartile\ Range}$, \}

The computations of the statistical analysis are computed using the following definitions.

$$A_{P-Sum} = \sum_{s=1}^{m} a_s$$

$$A_{P-Mean} = \left[\sum_{s=1}^{m} a_s\right] / m$$

$$A_{P-Geometric\ Mean} = \sqrt[m]{\left[\prod_{s=1}^{m} a_s\right]}$$

$$A_{P-Harmonic\ Mean} = \left[\left[\sum_{s=1}^{m} {a_s}^{-1}\right] / m\right]^{-1}$$

$$A_{P-Min} = Min\ (a_s)\ ;\ s \in [1, m]$$

$$A_{P-Max} = Min\ (a_s)\ ;\ s \in [1, m]$$

$$A_{P-Range} = [Min\ (a_s)\ , Min\ (a_s)]\ ;\ s \in [1, m]$$

$$A_{P-Variance} = \frac{1}{m-1}\sum_{s=1}^{m}(a_s - \bar{a})^2$$

$$Where\ \bar{a} = \left[\sum_{s=1}^{m} a_s\right]/m$$

$$A_{P-Standard\ deviation} = \sqrt{\frac{1}{m-1}\sum_{s=1}^{m}(a_s - \bar{a})^2}$$

$$Where\ \bar{a} = \left[\sum_{s=1}^{m} a_s\right]/m$$

$$A_{P-Skewness} = \frac{1}{(m-1)S^3}\sum_{s=1}^{m}(a_s - \bar{a})^3$$

$$Where\ S = \sqrt{\frac{1}{m-1}\sum_{s=1}^{m}(a_s - \bar{a})^2}$$

$$A_{P-Kurtosis} = \frac{1}{(m-1)S^4}\sum_{s=1}^{m}(a_s - \bar{a})^4$$

,

$$Where\ S = \sqrt{\frac{1}{m-1}\sum_{s=1}^{m}(a_s - \bar{a})^2}$$

$$A_{P-First\ Quartile} = \begin{cases} \dfrac{a_k + a_{k+1}}{2}; k \in whole\ number \\ a_k\ ; k \in fraction\ (Round\ fraction) \end{cases}$$

Where all $a_i's$ are arranged in ascending order and $k = (25 * m)/100$

$$A_{P-Third\ Quartile} = \begin{cases} \dfrac{a_k + a_{k+1}}{2}; k \in whole\ number \\ a_k\ ; k \in fraction\ (Round\ fraction) \end{cases}$$

Where all $a_i's$ are arranged in ascending order and $k = (75 * m)/100$

$$A_{P-Median} = \begin{cases} \dfrac{a_k + a_{k+1}}{2}; k \in even\ number \\ a_k\ ; k \in Odd\ Number \end{cases}$$

Where all $a_i's$ are arranged in ascending order and

$$k = \begin{cases} \dfrac{m}{2}; m \in even\ number \\ \dfrac{m+1}{2}\ ; m \in Odd\ Number \end{cases}$$

$$A_{P-Inter\ Quartile\ Range} = Q_3 - Q_1 = A_{P-Third\ Quartile} - A_{P-First\ Quartile}$$

It is observed from the analysis results obtained that all the analysis parameters provide no marked difference amongst the three classes considered hence the analysis results graphically exhibited per parameter extracted vary. The preliminary phase of the $MPECS$ contributes towards the $p_{Lesion-Area}$, $p_{Clr-Spread}$ and $p_{Lesion-Boundry}$ parameter extraction the three classes were analyzed based on the $A_{P-Range}$, $A_{P-Variance}$ and $A_{P-Standard\ deviation}$. The resulting graphs are as shown in Fig. 1,2 and 3 respectively.

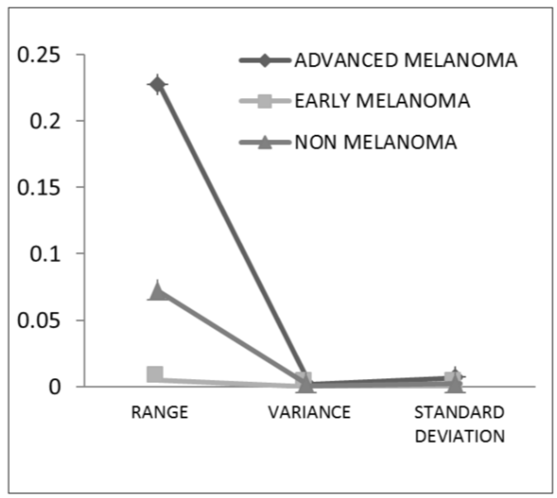

Fig 1 Statistical Analysis of $\boldsymbol{p_{Lesion-Area}}$

The second phase of the $\boldsymbol{MPECS}$ contributes the $\boldsymbol{p_{Lesion-Area}}$,$\boldsymbol{p_{Lesion-Bound}}$ and the $\boldsymbol{p_{Lesion-Eccent}}$ towards the construction of the parameter set $\boldsymbol{P}$. The results obtained are shown in Fig 4,5 and 6. The analysis result of the 3D projection of the skin lesions under test is shown in Fig 7.

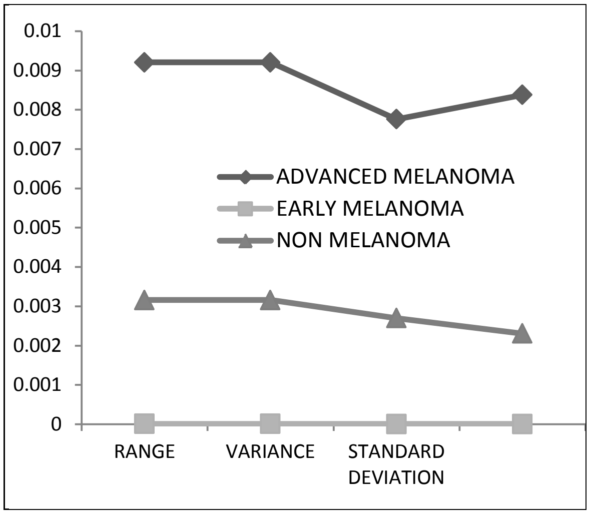

Fig 2: Statistical Analysis of $p_{Clr-Spread}$

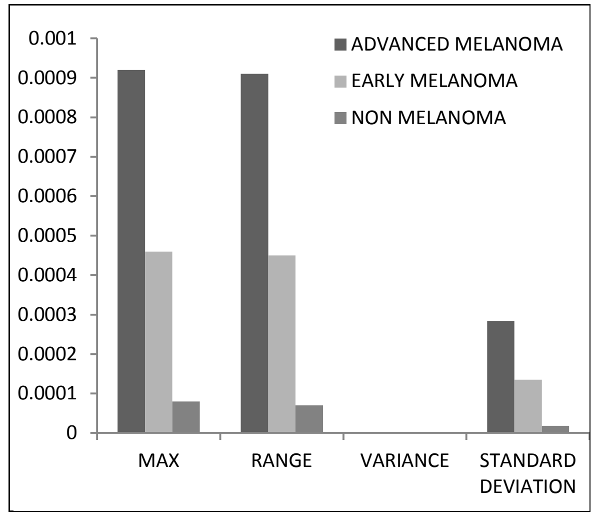

Fig 5 : Statistical Analysis of $p_{Lesion-Bound}$

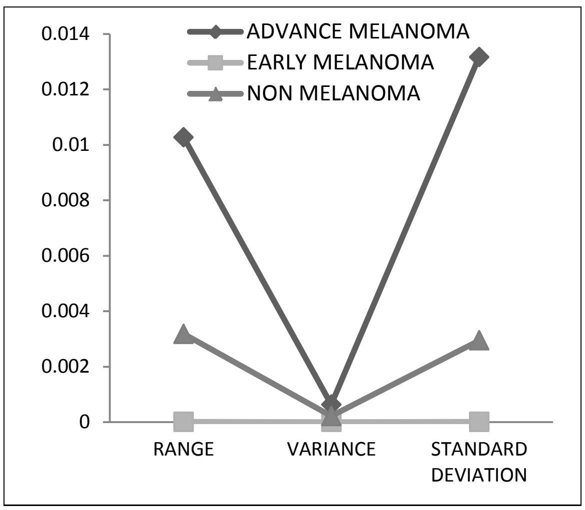

Fig 3 : Statistical Analysis of $p_{Lesion-Boundry}$

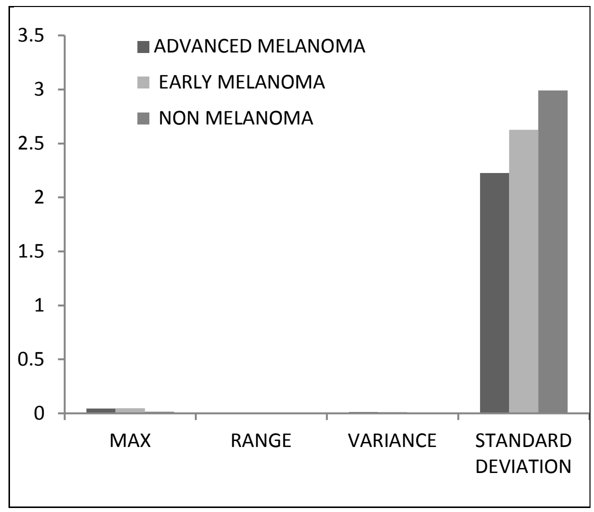

Fig 6 : Statistical Analysis of $p_{Lesion-Eccent}$

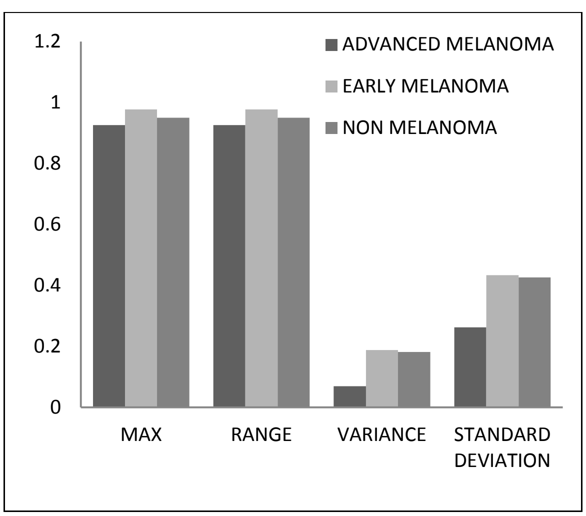

Fig 4 : Statistical Analysis of $p_{Lesion-Area}$

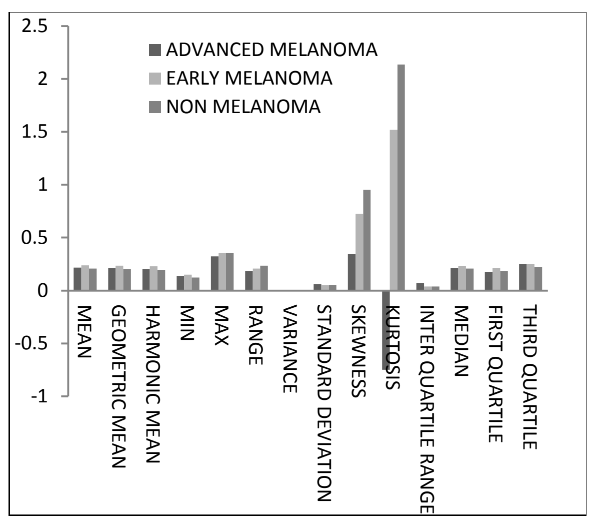

Fig 7 : Statistical Analysis of $p_{Lesion-3DDept}$

The color parameters defining the skin lesion in terms of the red channel , green channel and blue channel extracted from the data set are analyzed using the statistical methods discussed above and the results obtained are shown in Fig 8 and 9 for the $RChnl$, Fig 10 and 11 for the G_{Chnl} and Fig 12 and 13 for the B_{Chnl}. The parameters obtained from the fifth phase of the $MPECS$ and on analyzing the data the graphs deduced are shown in Fig 14 and 15.
The analysis of the parameters extracted from the phase six of the $MPECS$ using the dataset used in the evaluation is shown in Fig 16 and 17 for the hue channel. The saturation value channel analysis is shown in Fig 18, 19 and Fig 20 , 21. The parameters of the parameter set P are $p_{Hue_{Chnl}l-Mean}$, $p_{Hue_{Chnl}-Var}$, $p_{Saturation_{Chnl}-Mean}$, $p_{Saturation_{Chnl}-Var}$, $p_{Value_{Chnl}-Mean}$ and $p_{Value_{Chnl}-Var}$.

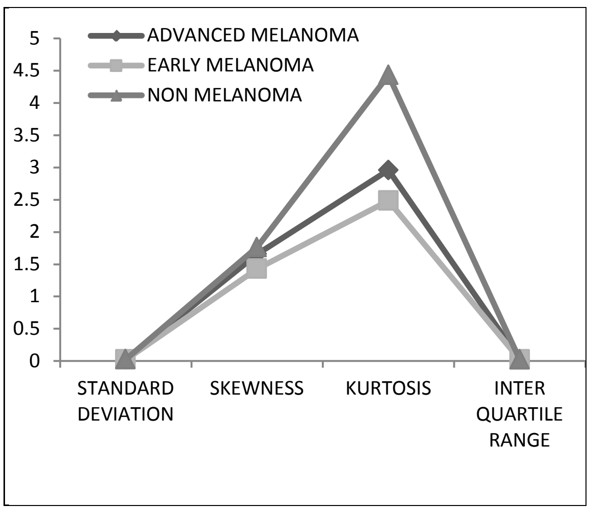

Fig 8 : Statistical Analysis of $\boldsymbol{p_{RChnl-Mean}}$

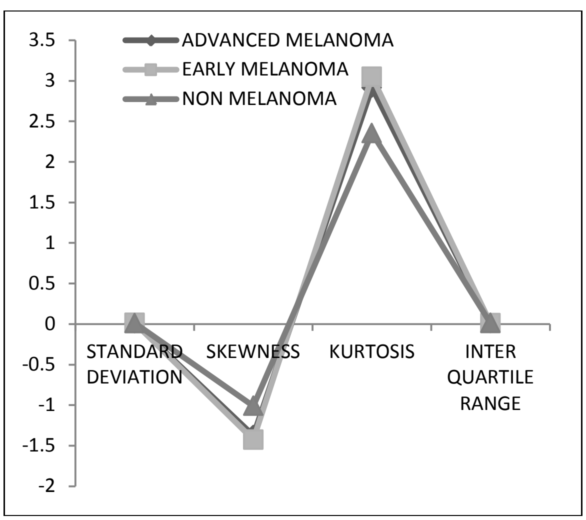

Fig 9 : Statistical Analysis of $\boldsymbol{p_{RChnl-Var}}$

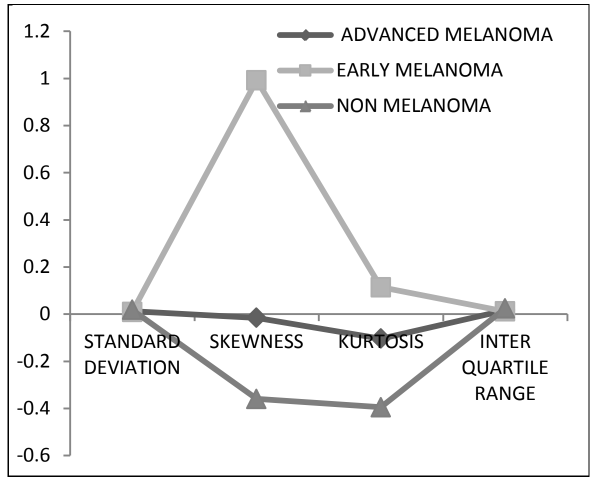

Fig 10 : Statistical Analysis of $\boldsymbol{p_{G_{Chnl}l-Mean}}$

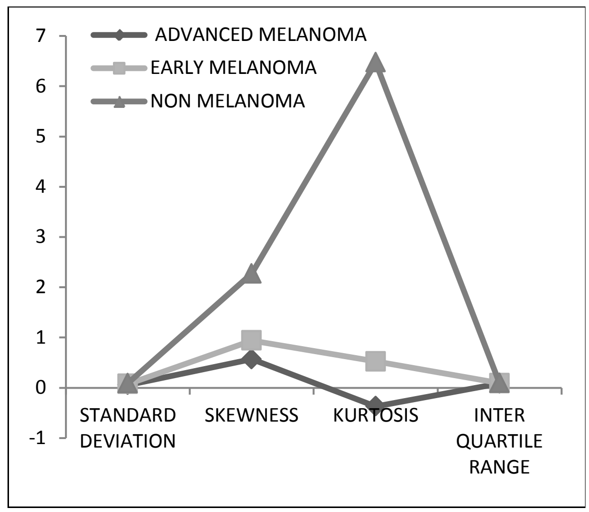

Fig 11 : Statistical Analysis of $\boldsymbol{p_{G_{Chnl}-Var}}$

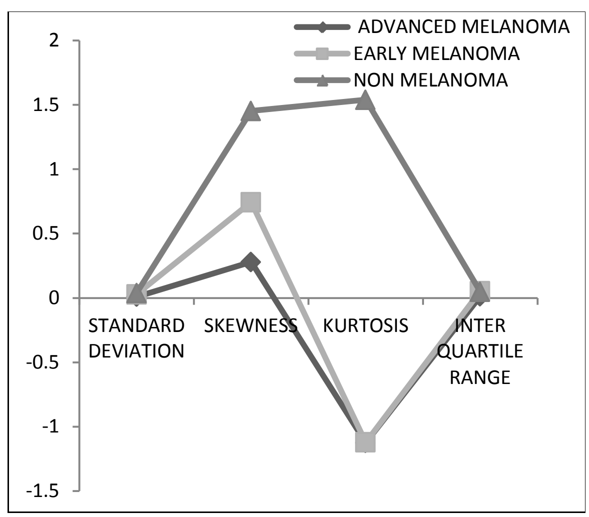

Fig 12 : Statistical Analysis of $\boldsymbol{p_{B_{Chnl}-Mean}}$

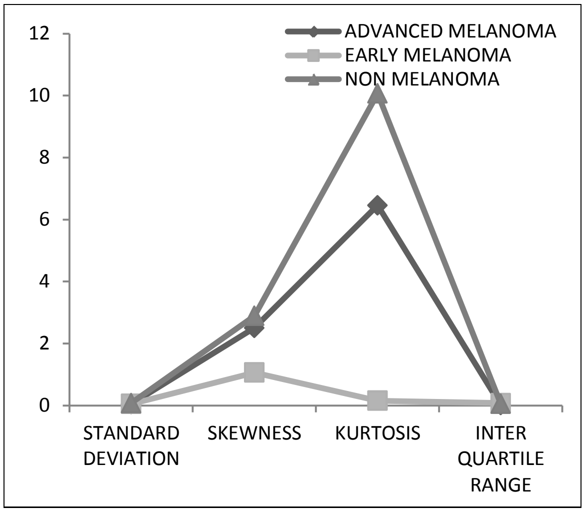

Fig 13 : Statistical Analysis of $p_{B_{Chnl}-Var}$

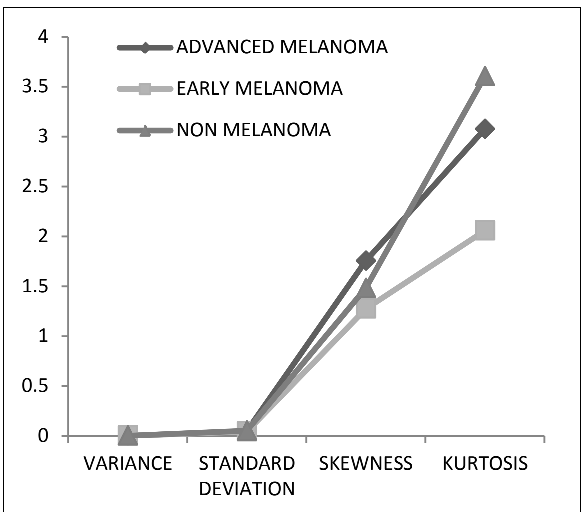

Fig 14 : Statistical Analysis of $p_{RChnl-Smooth}$

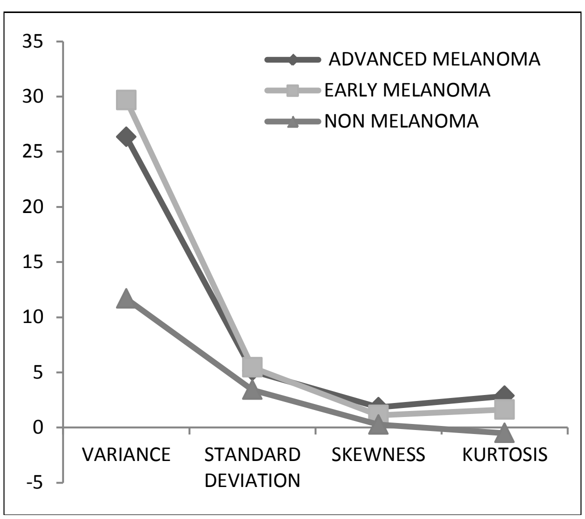

Fig 15 : Statistical Analysis of $p_{G_{Chnl}-Smooth}$

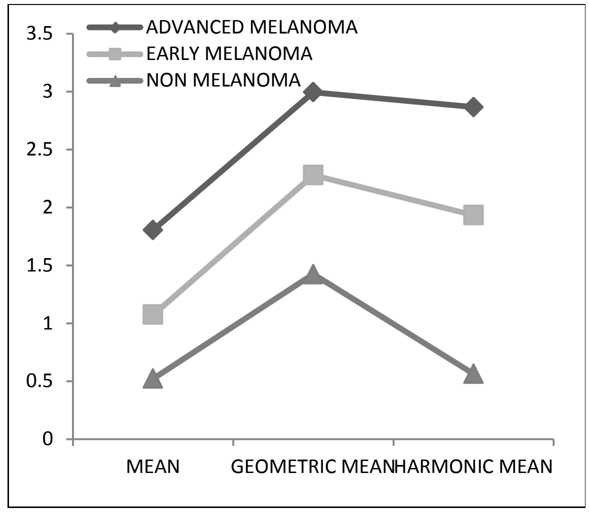

Fig 16 : Statistical Analysis of $p_{Hue_{Chnl}l-Mean}$

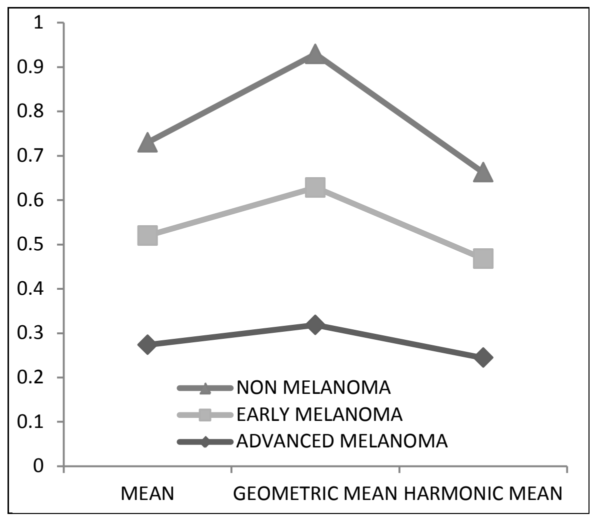

Fig 17 : Statistical Analysis of $p_{Hue_{Chnl}-Var}$

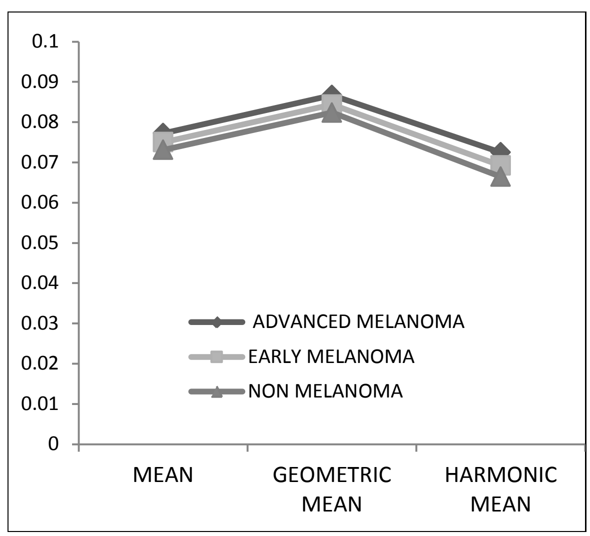

Fig 18 : Statistical Analysis of $p_{Saturation_{Chnl}-Mean}$

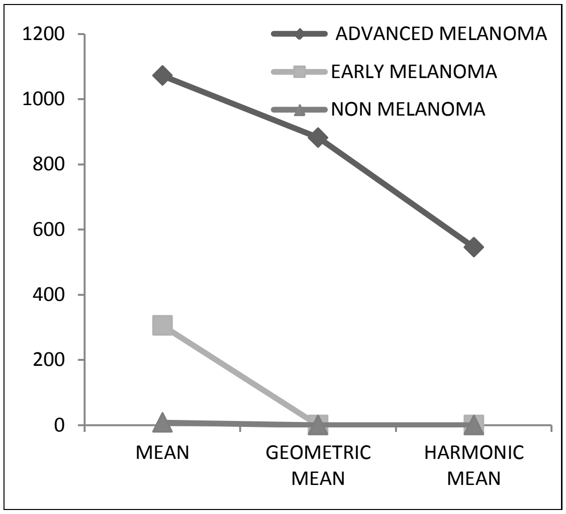

Fig 19 : Statistical Analysis of $p_{Saturation_{Chnl}-Var}$

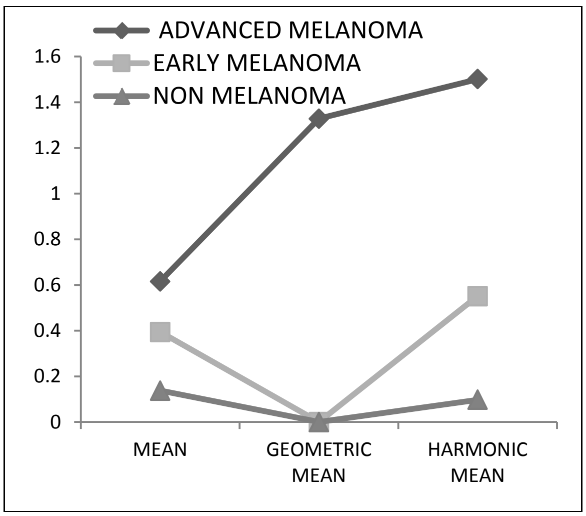

Fig 20 : Statistical Analysis of $p_{Value_{Chnl}-Mean}$

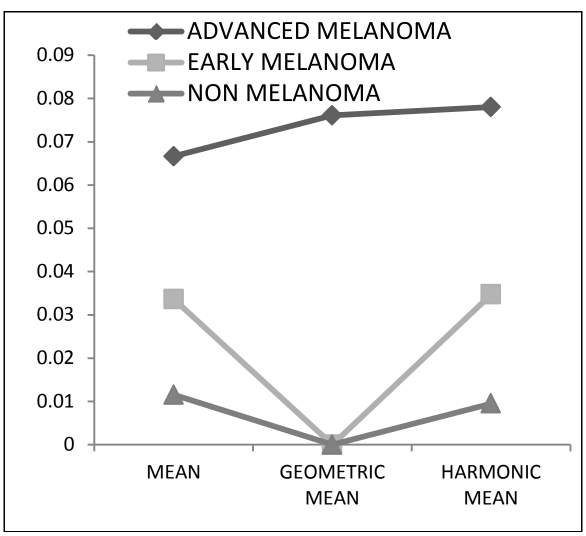

Fig 21 : Statistical Analysis of $p_{Value_{Chnl}-Var}$

From the results obtained it is clear that no singular statistical analysis and no single parameter extracted is sufficient to accurately classify the skin lesions of the data set into advanced melanoma, early melanoma and non melanoma classes. An advanced classification mechanism is to be incorporated in the $MPECS$ to accurately classify the skin lesions identified by ties parameters extracted. The use of neural networks, support vector machines and decision tree algorithms could be considered for classification.

5. Conclusion and Future Work

Skin cancer melanoma is life threatening and incurable in the advanced stages. It is complicated to identify the existence of melanoma in the nascent stages [20][21]. A Multi Parameter Extraction and Classification System – $MPECS$ is proposed in this paper to aid the early detection of in situ melanoma from dermoscopic images. The $MPECS$ defines an skin lesion as a set of extracted parameters or features. A multi phase approach is adopted in the extraction of the twenty one parameters extracted per dermoscopic image. The first phase extracts the symmetry of the skin lesion, the color spreading factor and the lesion boundary parameters. The area, perimeter and eccentricity of the skin lesion features are extracted in the second phase. The 3D projected depth parameter of the skin lesion is obtained from the third phase. The color parameters of the red, green and blue channels in terms of the mean and variance are obtained from the next phase. The mean and variance features of the red channel and green channel post the smoothening filter is obtained in the fifth phase. The last phase discusses the extraction of the hue , saturation and value channel parameter extraction procedures. The $MPECS$ is evaluated on a custom dataset created using the dermoscopic images obtained from the Atlas of Dermoscopy. This manuscript discusses the parameter extraction procedure adopted by the $MPECS$. The parameters extracted are exhaustive and the statistical analysis prove the need for advanced classification mechanisms to be adopted in the $MPECS$.
The future of the research work presented in this paper is to incorporate advanced classification systems using neural networks and to prove its efficiency over the existing computer aided melanoma detection and classification systems.

References

[1] American Cancer Society,"Cancer Facts and Figures 2012". 2012, American Cancer Society, Inc. pp 1-68
[2] Imran Ali, Waseem A. Wani and Kishwar Saleem,"Cancer Scenario in India with Future Perspectives",Cancer Therapy Vol 8, 56-70, 2011
[3] Sinha R,Anderson DE, Mc Donald SS and Greenwald P, "Cancer Risk and Diet in India",J Postgrad Med 2003,49:

222-228
[4] R. Marks, “Epidemiology of melanoma,” Clin. Exp. Dermatol., vol. 25, pp. 459–463, 2000
[5] World Health Organization, Ultraviolet Radiation and the INTERSUN Programme. (2007. Dec.). [Online]. Available: http://www.who.int/uv/faq/skincancer/en/
[6] R J. Pariser and D. M. Pariser, “Primary care physicians errors in handling cutaneous disorders,” J. Amer. Acad. Dermatol., vol. 17, pp. 239– 245, 1987
[7] Ilias Maglogiannis and Charalampos N. Doukas,"Overview of Advanced Computer Vision Systems for Skin Lesions Characterization",IEEE TRANSACTIONS ON INFORMATION TECHNOLOGY IN BIOMEDICINE, VOL. 13, NO. 5, SEPTEMBER 2009, pp 721-733
[8] I.M. Ariel, "Malignant Melanoma", Appleton-Century-Crofts, New York, 1981
[9] T. Gambichler, P. Regeniter, F. Bechara, A. Orlikov, R. Vasa, G. Moussa, M. Stücker, P. Altmeyer, and K. Hoffmann, “Characterization of benign and malignant melanocytic skin lesions using optical coherence tomography in vivo,” Journal of the American Academy of Dermatology, vol. 57, no. 4, pp. 629–637, 2007
[10] A. P. Dhawan, B. D’Alessandro, and X. Fu, “Optical imaging modalities for biomedical applications,” IEEE Reviews in Biomedical Engineering, vol. 3, pp. 69–92, 2010
[11] A. Goodson and D. Grossman, “Strategies for early melanoma detection: Approaches to the patient with nevi,” Journal of the American Academy of Dermatology, vol. 60, no. 5, pp. 719–735, 2009
[12] G. Argenziano, H. P. Soyer, S. Chimenti, R. Talamini, R. Corona, F. Sera, M. Binder, L. Cerroni, G. De Rosa, G. Ferrara, R. Hofmann-Wellenhof,M. Landthaler, S.W.Menzies, H. Pehamberger, D. Piccolo, H. S. Rabinovitz, R. Schiffner, S. Staibano, W. Stolz, I. Bartenjev, A. lum, R. Braun, H. Cabo, P. Carli, V. De Giorgi, M. G. Fleming, J. M. Grichnik, C. M. Grin, A. C. Halpern, R. Johr, B. Katz, R. O. Kenet, H. Kittler, J. Kreusch, J. Malvehy, G. Mazzocchetti, M. Oliviero, F. Ozdemir, K. Peris, R. Perotti, A. Perusquia, M. A. Pizzichetta, S. Puig, B. Rao, P. Rubegni, T. Saida, M. Scalvenzi, S. Seidenari, I. Stanganelli, M. Tanaka, K. Westerhoff, I. H. Wolf, O. Braun-Falco, H. Kerl, T. Nishikawa, K. Wolff, and A. W. Kopf, “Dermoscopy of pigmented skin lesions: Results of a consensus meeting via the Internet,” J. Amer. Acad. Dermatol., vol. 48, no. 5, pp. 680–693, 2003.
[13] M. E. Celebi, Y. A. Aslandogan,W. V. Stoecker, H. Iyatomi, H. Oka, and X. Chen, “Unsupervised border detection in dermoscopy images,” Skin Res. Technol., vol. 13, no. 4, pp. 454–462, 2007
[14] S. E. Umbaugh, R. H. Moss, and W. V. Stoecker, “An automatic color segmentation algorithm with application to identification of skin tumor borders,” Comput. Med. Imag. Graph., vol. 16, pp. 227–235, 1992
[15] V. T. Y. Ng, B. Y. M. Fung, and T. K. Lee, “Determining the asymmetry of skin lesion with fuzzy borders,” Comput. Biol. Med., vol. 35, pp. 103–120, 2005
[16] M. Elbaum, A. W. Kopf, H. S. Rabinovitz, R. Langley, H. Kamino, M. Mihm, A. Sober, G. Peck, A. Bogdan, D. Krusin, M. Greenebaum, S. Keem, M. Oliviero, and S. Wang, “Automatic differentiation of melanoma frommelanocytic nevi with multispectral digital dermoscopy: A feasibility study,” J. Amer. Acad. Dermatol, vol. 44, no. 2, pp. 207–218, 2001.
[17] G. Argenziano, G. Fabbrocini, P. Carli, V. De Giorgi, E. Sammarco, and M. Delfino, “Epiluminescence microscopy for the diagnosis of doubtful melanocytic skin lesions.Comparison of theABCDrule of dermatoscopy and a new 7-point checklist based on pattern analysis,” Arch. Dermatol., vol. 134, no. 12, pp. 1563–1570, 1998.
[18] G. Betta, G. Di Leo, G. Fabbrocini, A. Paolillo, and M. Scalvenzi, “Automated application of the “7-point checklist” diagnosis method for skin lesions: Estimation of chromatic and shape parameters,” in Proc. Instrum. Meas. Technol. Conf. (IMTC 2005), May, vol. 3, pp. 1818– 1822.
[19] M. Anantha, R. H. Moss, and W. V. Stoecker, “Detection of pigmented network in dermatoscopy images using texture analysis,” Comput. Med. Imag. Graph., vol. 28, pp. 225–234, 2004
[20] R. B. Mallet, M. E. Fallowfield, M. G. Cook, W. N. Landells, C. A. Holden, and R. A. Marsden, “Are pigmented lesion clinics worthwhile?” Br. J. Dermatol., vol. 129, pp. 689–693, 1993
[21] M. F. Healsmith, J. F. Bourke, J. E. Osborne, and R. A. C. Graham- Brown, “An evaluation of the revised seven-point checklist for the early diagnosis of cutaneous malignant melanoma,” Br. J. Dermatol., vol. 130, pp. 48–50, 1994
[22] Steven McDonagh, Robert B. Fisher and Jonathan Rees,"Using 3D information for classification of non-melanoma skin lesions",Available Online homepages.inf.ed.ac.uk/rbf/PAPERS/mcdonagh.pdf
[23] Brian D’Alessandro, Atam P. Dhawan,"3D Volume Reconstruction of Skin Lesions for Melanin and Blood Volume Estimation and Lesion Severity Analysis",IEEE Transactions on Medical Imaging, July 2012 DOI : 10.1109/TMI.2012.2209434
[24] M. Emre Celebi, Hassan A. Kingravia, Y. Alp Aslandogan, William V. Stoecker,"Detection of Blue-White Veil Areas in Dermoscopy Images Using Machine Learning Techniques",Proc. of SPIE Vol. 6144.doi: 10.1117/12.655779
[25] Marghoob AA, Braun RP, Kopf AW. Atlas of dermoscopy. London: Taylor & Francis; 2005
[26] Ru-Song Meng, Xiao Meng, Feng-Ying Xie and Zhi-Guo Jiang,"Early diagnosis for cutaneous malignant melanoma based on the intellectualized classification and recognition for images of melanocytic tumour by dermoscopy",Journal of Biomedical Graphics and Computing, December 2012, Vol. 2, No. 2. pp 37-47